

PRODUCTION OF STRONTIUM DOPED RICE HULL ASH SILICA BASED BIOACTIVE GLASS– ALGINATE COMPOSITE SCAFFOLDS AND *IN VITRO* SIMULATED BODY FLUID BEHAVIOUR

Kardelen Yangin¹, Ali Can Özarlan¹, Cem Batuhan Çevlik¹
Burcu Karakuzu İkizler¹, Sevil Yücel^{1*}

¹Department of Bioengineering, Faculty of Chemistry and Metallurgy, Yildiz Technical University, Istanbul, Turkey

Abstract. Bioactive glasses which contain silica as a major element (45%-60%; wt%) are used commonly due to its bioactivity and can be preferred in bone tissue engineering because of its behaviours in simulated body fluid (SBF) and ease of forming hydroxyapatite which comprises of 70% of bone. At the same time, alginate which is a natural biopolymer is an available choice from the perspective of biocompatibility and bioactivity due to ease of chemical modification, functionality and positive effects on stimulating and regenerating of bone tissue. In this study, Sr-doped rice hull ash (RHA) silica based bioactive glass which was produced via melt-quenching technique and alginate composite scaffolds were produced by using freeze-drying – lyophilization method. According to the bioactive (Hydroxyapatite formation) and biodegradable behavior (up to 7 days, swelling; 15% and up to 28 days, weight loss; 38%) analysis results, the composite scaffold in SBF show that these scaffolds can be a potential candidate for bone tissue engineering applications.

Keywords: alginate, bioactive glass, freeze drying, melt-quenching, Sr-doped, simulated body fluid.

Corresponding Author: Sevil Yücel, Professor, Department of Bioengineering, Faculty of Chemical and Metallurgical Engineering, Yildiz Technical University, Istanbul, Turkey, Tel.: +902123834628
e-mail: syucel@yildiz.edu.tr

Received: 24 May 2018; **Accepted:** 27 June 2018; **Published:** 31 August 2018

1. Introduction

Bones in the human body structure loss its functionality and undergo an irreversible change due to aging and various diseases. New generation artificial bone biomaterials are researched and improved in order to heal bone defects due to cracks, fractures and ruptures with this intention (Langer & Vacanti, 1993). A new alternative field, bone tissue engineering, serves as an approach to meet the needs of tedious bone surgeon operations via implants (Chen *et al.*, 2008; Place *et al.*, 2009). The major purpose of bone tissue engineering is turning back the diseased bone to its original biological and mechanical functionality. For this reason, there are ongoing researches about repair, regeneration and replace bone defects with bioactive scaffolds which are resembled to native bone structure, adhered to the bone and activated the genes for bone development. Bioactive scaffolds are engineered to biomimicry original bone structure (Badylak *et al.*, 2009; Mano *et al.*, 2007). Bioactive glasses are an attractive area about regeneration of bone tissue due to its biocompatibility, bioactivity, osteoconductivity and bone reproductivity properties. Especially these bioactive glasses are used for specific situations because of unavailability of bone implants to patients. Moreover, bioactive glasses adhere easily to the bone tissue and promote the formation of bone

tissue (Chen *et al.*, 2006; Xynos *et al.*, 2001; Boccaccini *et al.*, 2007; Jones *et al.*, 2007; Hench, 2006). Another key point about bioactive glasses is ease of production methods such as melt-quenching at high temperature and sol-gel process at low temperature (Hench, 1997).

A recent specific approach to bone tissue engineering is doping bone cell stimulant ions to the chemical composition of bioactive glasses. It has been known that strontium accelerates the healing period of bone disorders and has antibacterial characteristics. Therefore, strontium can be doped to bioactive glasses instead of calcium ions due to its charge and ionic diameter and plays a significant biological role in the bone repair and regeneration (Ortolani & Vai, 2006; Nielsen, 2004; Meunier *et al.*, 2004; Marie, 2005; Lao *et al.*, 2008). Ongoing researches about skeletal muscle tissue repair and regeneration have shown that growth factor delivery, cell transplantation or cooperation of more techniques with alginate are potential candidates for bone tissue engineering applications. Alginate scaffolds have positive effects on bone repair and regeneration because of their functionality to be introduced into the body in a minimally invasive manner, fill irregularly formed damages and the ease of chemical modification with adhesion ligands and controlled release of tissue induction factors (e.g., BMP, TGF- β) (Barralet *et al.*, 2005; Florczyk *et al.*, 2012; Lópiz-Morales *et al.*, 2010). The most common method to fabricate an alginate scaffold is freeze-drying - lyophilization technique, because homogeneous and excellent porous (~95%) scaffolds with highly anisotropic tubular structure and perfect interconnectivity within the pores can be achieved via freeze-drying technique (Laurencin *et al.*, 2002; Hutmacher & Cool, 2007). Additionally, the pore size can be controlled depends on the parameters such as phase separation temperature, solvent, polymer types and concentration of the polymer solution. Furthermore, scaffolds attained from this method generally demonstrate ordered tubular pores structures in the range of several hundred microns (>100 μm) and isotropic pore connectivity of smaller pore size (~ 10 μm) interconnected the large tubular pores diameters (Ma & Choi, 2001; Boccaccini & Maquet, 2003). The biocomposites of alginate with bioactive glass ceramics are extensively studied for bone repair due to increased mineralization and protein adsorption properties of bioactive glass in alginate. Moreover, human periodontal ligament fibroblast and osteosarcoma cells are viable, attached and proliferated effectively on the alginate-bioactive glass composite scaffolds compared to the reference alginate scaffolds (Srinivasan *et al.*, 2012).

Rice hull ash, which is an agricultural waste, contains plenty of silica in its content (about 60%). RHA is also cheap alternative source of amorphous silica. RHA based silica commonly uses lots of studies because of these properties (Yücel *et al.*, 2013). Furthermore, RHA based silica contains different elements such as copper, magnesium and iron that can play an important role in tissue healing (Özarlan & Yücel, 2016). In this study, Sr-doped RHA-silica based bioactive glasses were produced via melt-quenching technique at the chemical composition of weight which is 50% SiO₂ – 21% Na₂O – 22% CaO – 4% P₂O₅ – 3% SrO. Three different compositional alginates (2%; sodium alginate/water : g/ml) – RHA-silica based bioactive glass composite scaffolds which contain 1%, 2% and 3% w/v bioactive glasses, were fabricated utilizing from freeze-drying – lyophilization technique. Produced Sr-doped RHA-silica based bioactive glass composite scaffolds were tested with several characterization studies such as Fourier-transform infrared spectroscopy (FT-IR), scanning electron microscope (SEM), inductively coupled plasma-optical emission spectrometry (ICP-

OES) analysis to investigate of its morphological and chemical properties changes and to investigate bioactivity and biodegradability behaviour in simulated body fluid.

2. Materials and methods

2.1. Materials

Strontium oxide (SrO) and alginic acid sodium salt powder were purchased from Sigma Aldrich. Calcium carbonate (CaCO_3), sodium bicarbonate (NaHCO_3), di-sodium hydrogen phosphate dihydrate ($\text{Na}_2\text{HPO}_4 \cdot 2\text{H}_2\text{O}$) were supplied from Merck. For *in vitro* bioactivity and biodegradability tests, simulated body fluid was prepared by the Kokubo method (Kokubo & Takadama, 2006).

2.2. Production of RHA based silica (RS) from Sodium Silicate Solution

Sodium silicate solution (Na_2SiO_3) was obtained from rice hull ash according to alkali extraction method (Yucel *et al.*, 2013). Firstly, approximately 500 mL prepared sodium silicate solution was poured into a plastic beaker. The solution was gelled at pH 7 value with the help of 1 M hydrochloric acid (HCl). Obtained silica gel waited for 24 hours for the purpose of aging the gel. The gel was washed three times at each five minutes via centrifuge. The wet silica gels in watch glass were placed into the incubator at 80° C for 48 hours. The dried sample was ground by agate mortar. Further, silica powder was washed one more time to obtain well purified from sodium chloride salt or another ions, particles, foreign agents. Straightaway washed silica powder were dried at 80° C for 24 hours. The silica powder was grained second time using a grinding device (Retsch, PM 400) for 30 minutes at 200 rpm and then one hour at 250 rpm rotational speed. Thus, rice hull ash silica powder was successfully obtained with desired particle size (<50 μm).

2.3. Production of Sr-doped RHA-silica based bioactive glass (Sr-RSBG)

Mixture of chemicals (RHA based silica-SrO- CaCO_3 - NaHCO_3 - $\text{Na}_2\text{HPO}_4 \cdot 2\text{H}_2\text{O}$) were put together in a platinum pot. Then platinum pot was put in the muffle furnace (Protherm Furnaces) for 1 hour at 1400°C. Immediately, the melted mixture was cast into the cold water bath. After, bioactive glasses were ground roughly in order to enhance homogenization. Subsequently, dry bioactive glass particles were put in a platinum pot and they were maintained at muffle furnace for 2 hours at 1450°C in order to strengthen the bioactive glass effectively. At the end of 2 h, samples were cast again onto the counter and annealed at 550 °C for 24 h in a furnace. Finally, in order to get suitable particles for the scaffold production, the bioactive glasses were ground by using grinding device (Retsch, PM 400). The bioactive glasses were placed into the agate cells and they were kept in device for 30 minutes at 200 rpm and 1 hour at 250 rpm to obtain the desired particle size which is under 50 μm . The bioactive glasses were acquired for the following procedure.

2.4. Fabrication of composite scaffolds

The scaffolds were produced via freeze-drying method. In the first instance, 1 g Na-Alginate powder was dissolved in 50 ml distilled water by stirring at room temperature for 2 hours to obtain a homogenous 2% w/v of alginate stock solution. At the end of 2 hours, 10 ml 2% w/v of alginate stock solution were mixed with bioactive glasses 1%, 2% and 3% w/v; g/mL, in beaker respectively. Correspondingly, 0.1g, 0.2g

and 0.3g bioactive glass powders were put in beakers which involves alginate solution and stirred for 2 hours. Subsequently, approximately 200 μm of the bioactive glass powder - alginate mixture was transferred into each of the well of a 96 well-plate. They were incubated at -20°C for 4 days in order to make pre-freezing. Finally, they were freeze-dried by using a lyophilizer at -80°C for 2 days. Thus, bioactive glass-alginate composite scaffolds were successfully obtained. Composition and abbreviation of scaffolds were given in Table 1.

Table 1. Composition and abbreviation of scaffolds

	<i>Alginate</i> (w/v %)	<i>Bioactive</i> <i>glass/Alginate solution</i> (w/v %)	<i>Water content</i> (ml)
Sr-RSBGAS* -1	2	1	100
Sr-RSBGAS* -2	2	2	100
Sr-RSBGAS* -3	2	3	100

*Sr-RSBGAS: Sr-doped RHA-silica based bioactive glass/alginate composite scaffold

2.5. Investigation of *in vitro* SBF behavior for composite scaffold

In vitro SBF studies were applied for each scaffold in SBF. The scaffolds were soaked in 24.5 mL of SBF for 7, 14, 21 and 28 days, stored and dried in an incubator at a specified temperature at $37 \pm 1^{\circ}\text{C}$, which was the closest value to the body temperature.

The scaffolds were immersed in newly prepared SBF in every seven days. RHA based silica, RHA-silica based bioactive glass and composite scaffolds (the presence of chemical functional groups in scaffolds, before and after simulated body fluid -SBF-immersion) were characterized using FT-IR (Shimadzu) in attenuated total reflection (ATR) mode using an ATR cell with a diamond reflection element, between the range of 4000 cm^{-1} and 650 cm^{-1} . Scaffolds were mounted directly onto the surface of ATR crystal. These data were gathered up in transmittance mode.

The morphology of scaffolds was investigated with scanning electron microscope (SEM, Zeiss Evo@Ls 10) before and after the scaffolds were soaked in SBF. Structural characterization was determined and interpreted via SEM images. Scaffolds were covered with gold via a Sputter Coater device (Emitech K 550X) and images were obtained for the analysis.

Si, Ca, Na, P and Sr ion changes of stored SBF samples in 28 days period were determined by using an inductively coupled plasma optical emission spectrometry (ICP-OES, Shimadzu Icp-9000) at 27.12 MHz frequency and 167 nm to 800 nm wavelength range.

Swelling studies were carried out by using SBF for scaffolds. They were immersed in SBF at 37°C for 4 and 7 days. Swelling ratio was measured utilizing from the equation;

$$\text{Swelling Ratio} = [(w_w - w_d) / w_d] \quad (1)$$

where w_w and w_d are wet and dry weight of the scaffolds, respectively.

In vitro degradation studies were performed by using SBF. 3 different compositional scaffolds were immersed in SBF for 7, 14, 21 and 28 days and they were dried at 37°C . Their wet and dry weights were recorded before and end of these days and degradation rate, also known as rate of weight loss, were calculated with the following equation;

$$(\text{rate of weight loss } \%) = [(w_i - w_t) / w_i] \times 100 \quad (2)$$

where w_i and w_t represent initial and terminal (dry) weights of scaffolds for every 7 days, respectively.

3. Results and discussion

3.1. FT-IR Analysis

The comparative FT-IR spectra of RHA based silica and Sr-doped RHA-silica based bioactive glass were given in Figure 1(A). FT-IR analysis of RS demonstrates that the dense peak of Si – O bends between the range of $1000 - 1100 \text{ cm}^{-1}$ and O – H bends around 3500 cm^{-1} due to the water content in silica. In addition, FT-IR characterization of Sr-RSBG shows that the large peak of Si – O – Si bends around 900 cm^{-1} , Si – O bends around 1100 cm^{-1} and O – H bonds between the range of 3200 cm^{-1} and 3600 cm^{-1} due to water absorption capacity (Stuart, 2004). Fig. 1(B) shows the FT-IR spectra of all scaffold in comparison to bioactive glass and alginate structure before immersed in SBF. FT-IR analyses prove that the presence of bioactive glass and alginate in bioactive glass composite scaffold. Si – O bends between the range of $1000 - 1100 \text{ cm}^{-1}$ and Si – O – Si bends around 900 cm^{-1} resembles the peaks of bioactive glass hence proves it. Furthermore, dense O – H peaks between the range of 3200 cm^{-1} and 3600 cm^{-1} due to water absorption capacity, C – O bonds between the range of 1400 cm^{-1} and 1600 cm^{-1} and around 1000 cm^{-1} demonstrate that the resemblance of alginate structure and bioactive glass composite scaffold, therefore, prove the presence of alginate in this bioactive glass composite scaffold (Stuart, 2004).

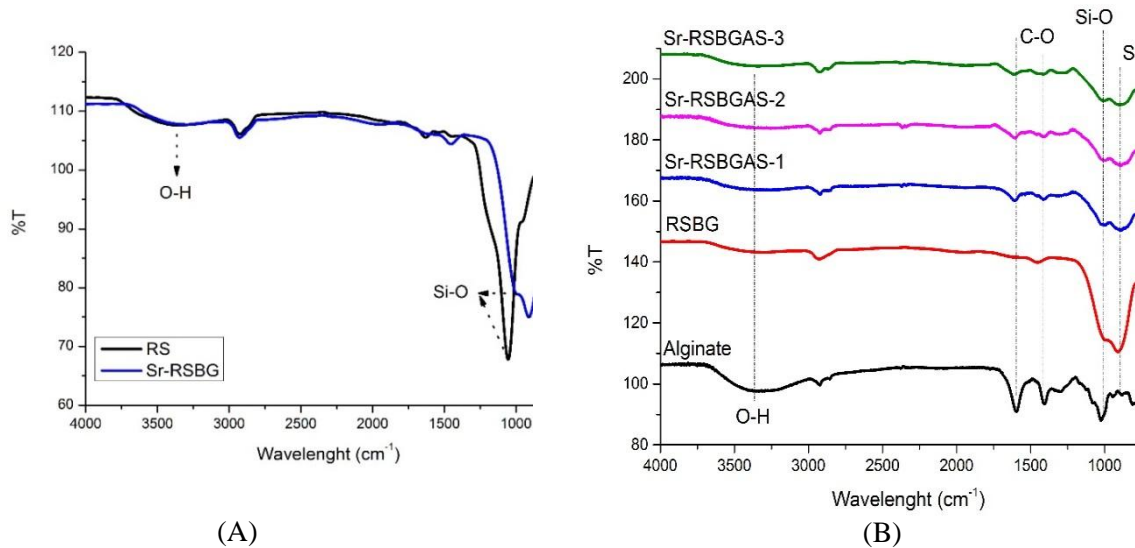


Figure 1. FT-IR graphs comparison; (A): RS and Sr-RSBG samples, (B): Alginate, RSBG and all scaffolds samples

In Fig. 2, the difference between composite scaffolds is shown before and after immersing in SBF. Large peaks of O – H between the range of 3200 cm^{-1} and 3600 cm^{-1} and C – O bonds between the range of 1400 cm^{-1} and 1600 cm^{-1} resemble due to the structural components but increasing P – O peaks between the range of 650 cm^{-1} and

1140 cm^{-1} and decreasing Si – O bends between the range of 1000 – 1100 cm^{-1} and Si – O – Si bends around 900 cm^{-1} demonstrates that the formation of hydroxyapatite (HA) layer (Stuart, 2004; Yucel *et al.*, 2013; Özarlan & Yücel, 2016). At the same time, FT-IR analysis of 3 composite scaffolds before and 7 days immersed in SBF proves the difference between these scaffolds and formation of new chemical structures. High density of P – O peaks between the range of 650 cm^{-1} and 1140 cm^{-1} and low density of Si – O bends between the range of 1000 – 1100 cm^{-1} and Si – O – Si bends around 900 cm^{-1} show the difference between before and after immersing in SBF. P – O vibration due to the presence of a crystalline calcium phosphate apatite has not seen clearly in Sr-RSBGAS-1 because of less bioactive glass compared to Sr-RSBGAS-2 and Sr-RSBGAS-3. Also O – H bonds between the range of 3200 cm^{-1} and 3600 cm^{-1} demonstrate perfect water absorption capacity (Stuart, 2004; Yucel *et al.*, 2013; Ozarlan & Yucel, 2016).

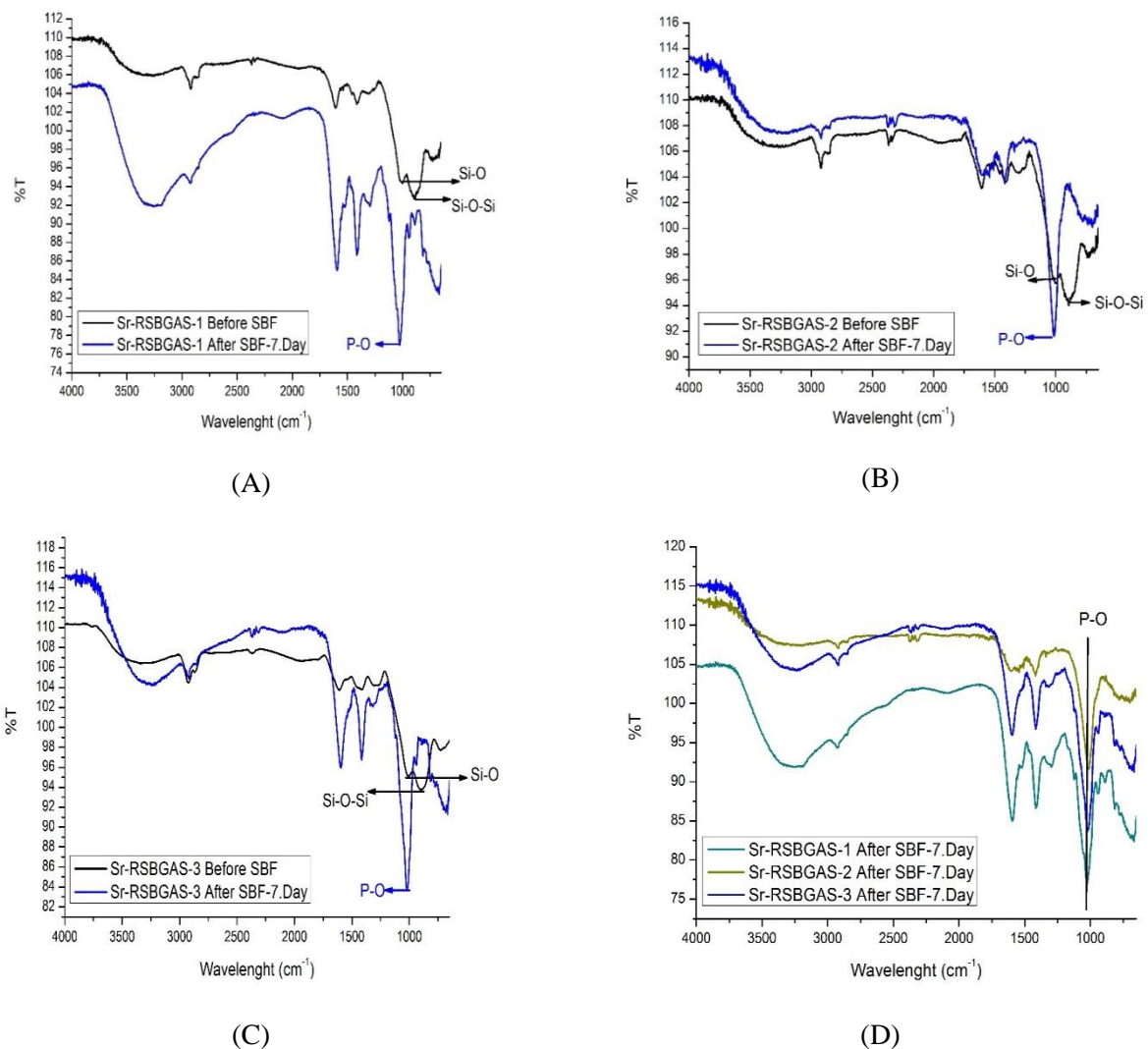
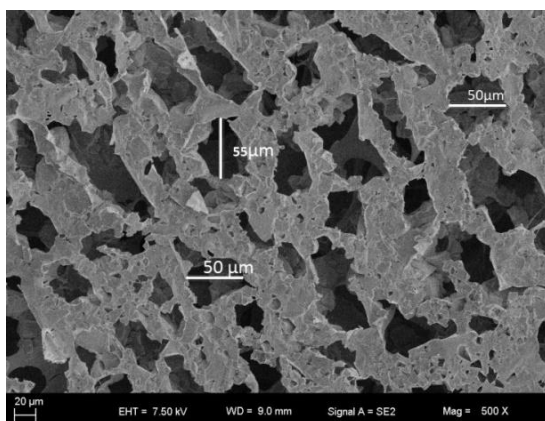


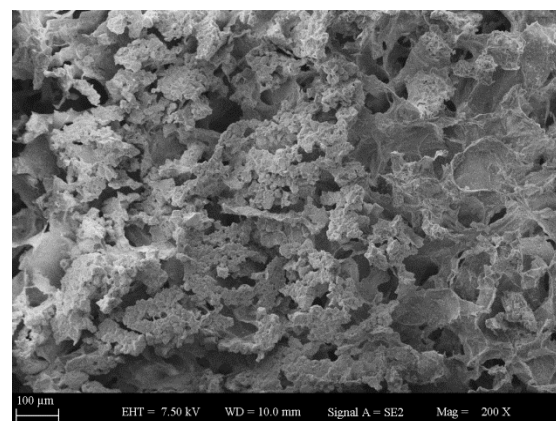
Figure 2. FT-IR graphs comparison; (A): Sr-RSBGAS-1 before and after SBF (7.Day), (B): Sr-RSBGAS-2 before and after SBF (7.Day), (C): Sr-RSBGAS-3 before and after SBF (7.Day), (D): All scaffolds after SBF immersion for 7 days

3.2. SEM Analysis

SEM images illustrate the 3 different bioactive glass composite scaffolds before and after immersing in SBF. All SEM images demonstrate dense porous structures of scaffolds effectively due to freeze-drying method. The diameter of the pores is larger in Sr-RSBGAS-3 (Fig. 3(E)) as compared to Sr-RSBGAS-1 (Fig. 3(A)) and Sr-RSBGAS-2. The average pore diameter is 53, 80 and 90 μm for Sr-RSBGAS-1, Sr-RSBGAS-2 and Sr-RSBGAS-3, respectively. A pore diameter of 90 μm may be acceptable for bone regeneration because optimum pore size of 100 – 350 μm is considered to be available for bone tissue engineering applications (Karageorgiou & Kaplan, 2005). Moreover, porous structure continues within a synthetic matrix. This is a key point for the nutrition transport, angiogenesis, cell migration and proliferation (Mooney *et al.*, 1996). The pores are well inter-connected as seen from the images (Fig. 3). A huge surface area supports cell attachment, connectivity and growth and great pore size. These features are necessary for accommodate and subsequently transport nutrition for cells in order to repair the damaged tissue at the same time (Srinivasan *et al.*, 2012). Therefore, pore size and interconnectivity should be controlled and tuned carefully for bone regeneration. The surface morphology of the different compositional bioactive glass composite scaffolds which (Fig. 3(B)) indicates Sr-RSBGAS-1, (Fig. 3(D)) indicates Sr-RSBGAS-2 and (Fig. 3(F)) indicates Sr-RSBGAS-3, shows the typical characteristics of apatite precipitation on the surfaces after immersion in SBF. Usually, apatite precipitation initiates with the formation of individual granules, which then gradually grow to form a dense layer on the surface of the sample. HA layer covered all over the surface of the bioactive glass composite scaffolds with increasing in immersion time from 7 days to 28 days (Naik *et al.*, 2016). Accumulation of an HA-rich layer on the surface of the scaffolds is fundamental for the cell and extracellular matrix in order to make direct bonding of the scaffolds in bone tissue engineering applications (Srinivasan *et al.*, 2012). Furthermore, HA formation is significant for attachment to the native bone structure. However, there is a difference between the scaffolds due to ratio of bioactive glass in the scaffolds. As seen from the Fig. 3, the apatite formation increases gradually from Sr-RSBGAS-1 to Sr-RSBGAS-3. This result proves that increasing ratio of bioactive glass influence positively to formation and accumulation of HA layer. In Fig. 3(B), HA formation changes part by part of the scaffold, however, in the same Fig. 3(F), apatite formation is observed effectively due to high bioactive glass ratio compared to 1% composite scaffold. Additionally, there are some factors that affect the growth rate of the apatite layer such as temperature and ion concentration (Yucel *et al.*, 2013).



(A)



(B)

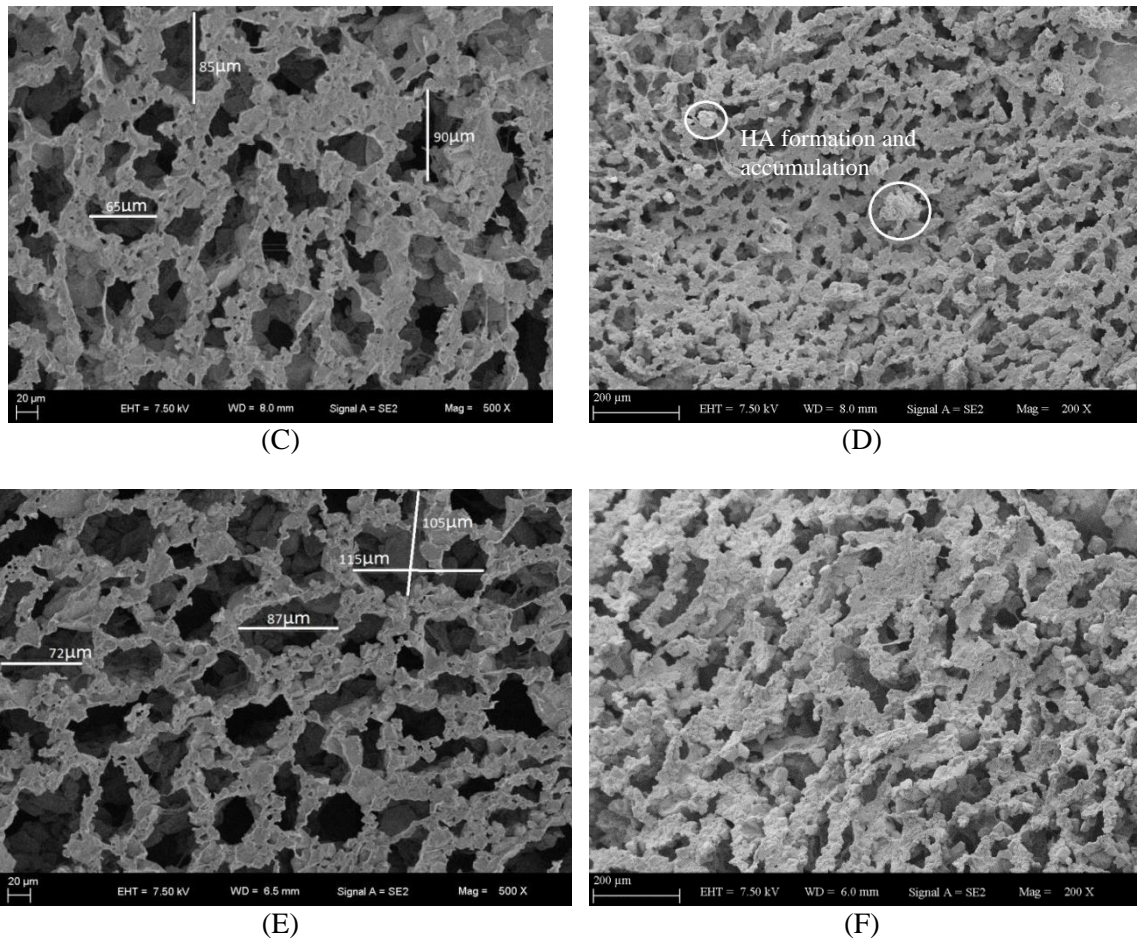


Figure 3. Composite scaffolds SEM images, before and after 28 day immersion in SBF, respectively; (A-B): Sr-RSBGAS-1, (C-D): Sr-RSBGAS-2, (E-F): Sr-RSBGAS-3

3.3. ICP-OES Analysis

To investigate the bioactivity and biodegradability properties due to ion release, the ions (Si, Ca, Na, P and Sr) changing values between composite scaffolds and SBF for 28 days were determined by ICP-OES analysis and the results were shown in Fig. 4. According to ICP-OES results, all scaffolds release rapidly ions into SBF throughout 14 days. The rapid release from scaffolds is related to the biodegradation of scaffolds. Furthermore, Strontium is also a factor of rapid dissolution. Especially, the slow increase of ion release (Ca and P) between the 14th and 21st days indicates that the HA formation takes place at a faster rate. A nearly constant release of Ca and P ions between the 14th and 21st days is related Ca-P precipitation (HA formation step) on scaffolds surface.

3.4. *In vitro* swelling and degradation studies of scaffolds

Swelling and degradation changes of immersed scaffolds in SBF were given in Fig. 5. The swelling ratios of scaffolds almost close to the values of the literature except for Sr-RSBGAS-1 (Naik *et al.*, 2016). Sr-RSBGAS-1 has a higher ratio of alginate, therefore, it has not strong, cross-linked bonds inside so may be dissolved and the swelling ratio will be higher than other composite scaffolds. *In vitro* degradation studies was performed in SBF for 7, 14, 21 and 28 days at $37\pm 1^\circ\text{C}$. The degradation rate is

calculated from initial and terminal weights of the scaffolds before and after soaking in SBF in comparison to different periods. The degradation rate of the scaffolds is similar to another observation (Naik *et al.*, 2016). The degradation rate is significant from biodegradation and matching the rate of tissue regeneration (Srinivasan *et al.*, 2012). The results illustrate that the scaffolds are biodegradable for the perspective of tissue engineering.

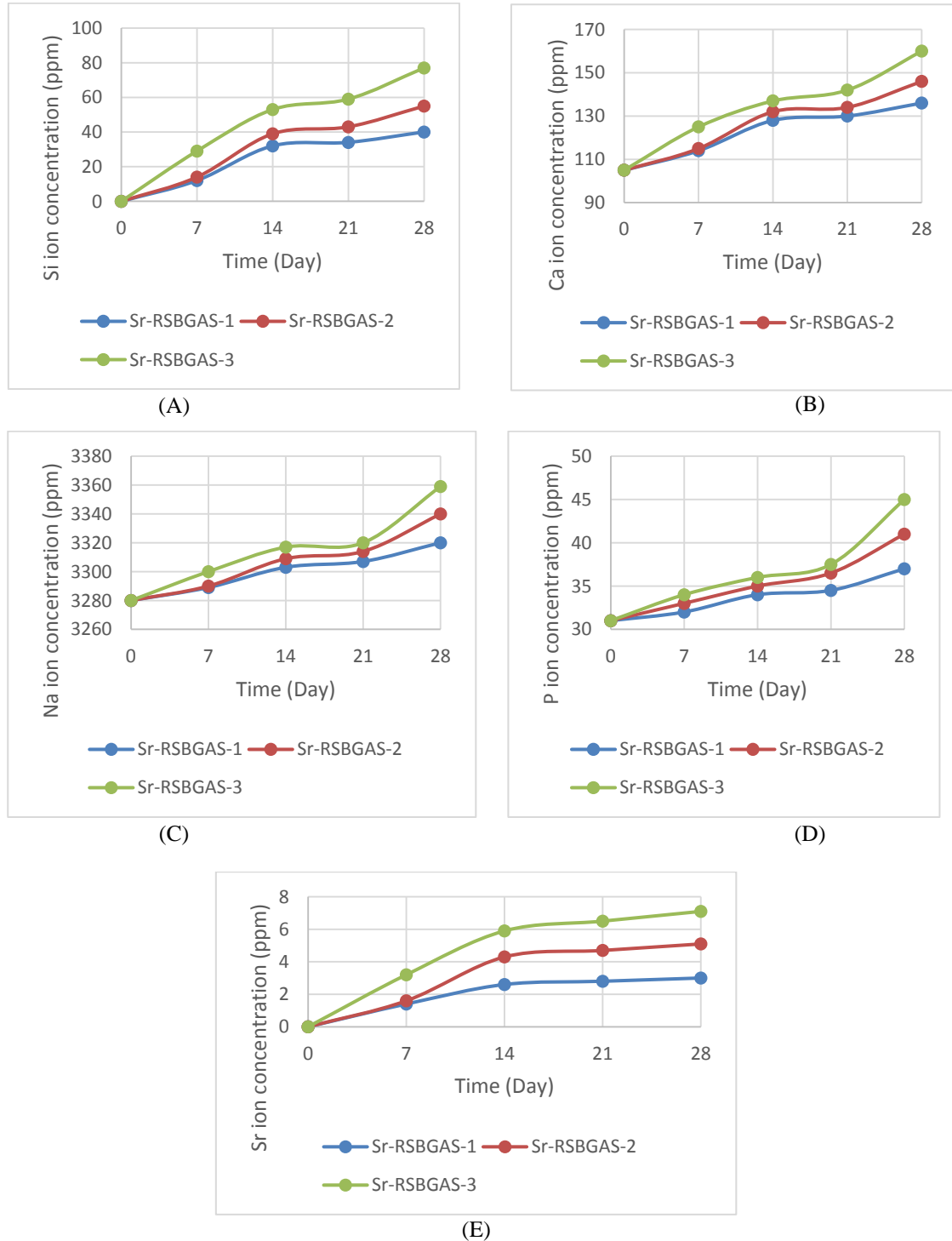
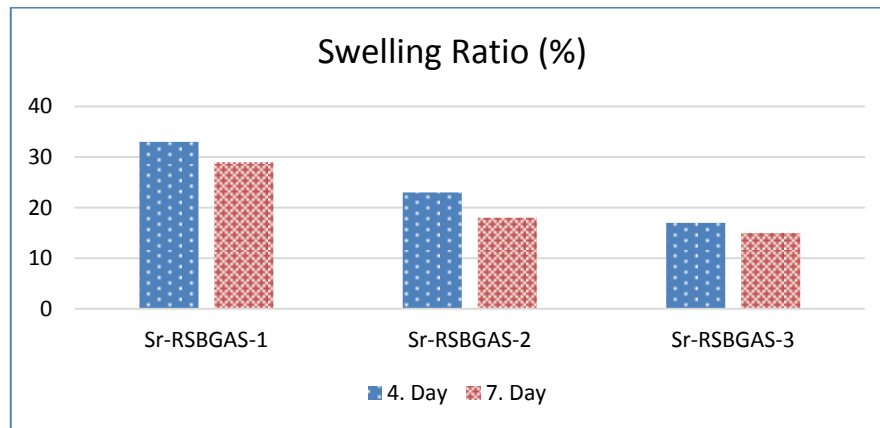
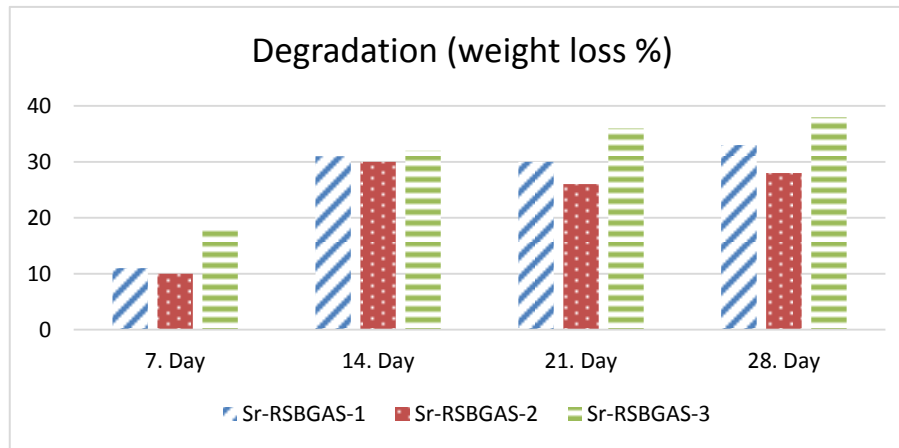


Figure 4. Ion changes of immersed composite scaffolds in SBF for 28 days; (A): Si ion changes, (B):Ca ion changes, (C):Na ion changes, (D):P ion changes, (E):Sr ion changes



(A)



(B)

Figure 5. Swelling ratio (%) graph (A) and degradation (%) graph (B) of scaffolds after SBF soaking for various time periods; A:swelling ratio (%) – time (days; 4, 7) graph of scaffolds, B: degradation (%) – time (day; 7,14,21,28) graph of scaffolds

4. Conclusion

Sr-doped RHA-silica based bioactive glass – alginate composite scaffolds were proved to have suitable properties to facilitate bone regeneration by an understanding of SBF studies and its behavior inside SBF. Also, the three different compositional scaffolds which are, Sr-RSBGAS-1, Sr-RSBGAS-2 and Sr-RSBGAS-3 had a pore diameter of about 53, 80 and 90 μm , respectively with exhibited controlled porosity with freeze-drying technique and swelling ability, limited degradation and enhanced biomineralization.

References

Badylak, S.F., Freytes, D.O. & Gilbert, T.W. (2009). Extracellular matrix as a biological scaffold material: structure and function, *Actabiomaterialia*, 5, 1-13.

- Barralet, J., Wang, L., Lawson, M., Triffitt, J., Cooper, P. & Shelton, R. (2005). Comparison of bone marrow cell growth on 2D and 3D alginate hydrogels, *Journal of Materials Science: Materials in Medicine*, 16, 515-519.
- Boccaccini, A.R., Chen, Q., Lefebvre, L., Gremillard, L. & Chevalier, J. (2007). Sintering, crystallisation and biodegradation behaviour of Bioglass[®]-derived glass-ceramics, *Faraday discussions*, 136, 27-44.
- Boccaccini, A.R. Maquet, V. (2003). Bioresorbable and bioactive polymer/Bioglass composites with tailored pore structure for tissue engineering applications, *Composites Science and Technology*, 63, 2417-2429.
- Chen, Q., Roether, J. & Boccaccini, A. (2008). Tissue engineering scaffolds from bioactive glass and composite materials, *Topics in tissue engineering*, 4, 1-27.
- Chen, Q.Z., Thompson, I.D. & Boccaccini, A.R. (2006). 45S5 Bioglass-derived glass-ceramic scaffolds for bone tissue engineering, *Biomaterials*, 27, 2414-2425.
- Florczyk, S.J., Leung, M., Jana, S., Li, Z., Bhattarai, N., Huang, J.I., Hopper, R.A. & Zhang, M. (2012). Enhanced bone tissue formation by alginate gel-assisted cell seeding in porous ceramic scaffolds and sustained release of growth factor, *Journal of Biomedical Materials Research Part A*, 100, 3408-3415.
- Hench, L.L. (1997). Sol-gel materials for bioceramic applications, *Current Opinion in Solid State and Materials Science*, 2, 604-610.
- Hench, L.L. (2006). The story of Bioglass, *Journal of Materials Science: Materials in Medicine*, 17, 967-978.
- Hutmacher, D. Cool, S. (2007). Concepts of scaffold-based tissue engineering—the rationale to use solid free-form fabrication techniques, *Journal of cellular and molecular medicine*, 11, 654-669.
- Jones, J.R., Gentleman, E. & Polak, J. (2007). Bioactive glass scaffolds for bone regeneration, *Elements*, 3, 393-399.
- Karageorgiou, V., Kaplan, D. (2005). Porosity of 3D biomaterial scaffolds and osteogenesis, *Biomaterials*, 26, 5474-5491.
- Kokubo, T., Takadama, H. (2006). How useful is SBF in predicting in vivo bone bioactivity?, *Biomaterials*, 27, 2907-2915.
- Langer, R., Vacanti, J.P. (1993). Tissue engineering, *Science*, 260, 920-926.
- Lao, J., Jallot, E. & Nedelec, J.M. (2008). Strontium-delivering glasses with enhanced bioactivity: a new biomaterial for antiosteoporotic applications?, *Chemistry of Materials*, 20, 4969-4973.
- Laurencin, C., Lu, H. & Khan, Y. (2002). Processing of polymer scaffolds: polymer-ceramic composite foams, *Methods of tissue engineering*, 705-714.
- López-Morales, Y., Abarrategi, A., Ramos, V., Moreno-Vicente, C., López-Durán, L., López-Lacomba, J.L. & Marco, F. (2010). In vivo comparison of the effects of rhBMP-2 and rhBMP-4 in osteochondral tissue regeneration, *Eur. Cell. Mater.*, 20, 78.
- Ma, P.X., Choi, J.W. (2001). Biodegradable polymer scaffolds with well-defined interconnected spherical pore network, *Tissue engineering*, 7, 23-33.
- Mano, J. Silva, G. Azevedo, H.S. Malafaya, P. Sousa, R. Silva, S. Boesel, L. Oliveira, J.M. Santos, T. & Marques, A. (2007). Natural origin biodegradable systems in tissue engineering and regenerative medicine: present status and some moving trends, *Journal of the Royal Society Interface*, 4, 999-1030.
- Marie, P.J. (2005). Strontium as therapy for osteoporosis, *Current opinion in pharmacology*, 5, 633-636.
- Meunier, P.J., Roux, C., Seeman, E., Ortolani, S., Badurski, J.E., Spector, T.D., Cannata, J., Balogh, A., Lemmel, E.-M. & Pors-Nielsen, S. (2004). The effects of strontium ranelate on the risk of vertebral fracture in women with postmenopausal osteoporosis, *New England Journal of Medicine*, 350, 459-468.

- Mooney, D.J., Baldwin, D.F., Suh, N.P., Vacanti, J.P. & Langer, R. (1996). Novel approach to fabricate porous sponges of poly (D, L-lactic-co-glycolic acid) without the use of organic solvents, *Biomaterials*, 17, 1417-1422.
- Naik, K., Chandran, V.G., Rajashekar, R., Waigaonkar, S. & Kowshik, M. (2016). Mechanical properties, biological behaviour and drug release capability of nano TiO₂-HAp-Alginate composite scaffolds for potential application as bone implant material, *Journal of Biomaterials Applications*, 31, 387-399.
- Nielsen, S.P. (2004). The biological role of strontium, *Bone*, 35, 583-588.
- Ortolani, S., Vai, S. (2006). Strontium ranelate: an increased bone quality leading to vertebral antifracture efficacy at all stages, *Bone*, 38, 19-22.
- Ozarslan, A.C., Yucel, S. (2016). Fabrication and characterization of strontium incorporated 3-D bioactive glass scaffolds for bone tissue from biosilica, *Materials Science and Engineering C*, 68, 350-357.
- Place, E.S., Evans, N.D. & Stevens, M.M. (2009). Complexity in biomaterials for tissue engineering, *Nature materials*, 8, 457.
- Srinivasan, S., Jayasree, R., Chennazhi, K., Nair, S. & Jayakumar, R. (2012). Biocompatible alginate/nano bioactive glass ceramic composite scaffolds for periodontal tissue regeneration, *Carbohydrate Polymers*, 87, 274-283.
- Stuart, B. (2004). *Infrared spectroscopy: fundamentals and applications*. John Wiley & Sons, Ltd. ISBNs: 0-470-85427-8 (HB). 0-470-85428-6 (PB).
- Xynos, I.D., Edgar, A.J., Buttery, L.D., Hench, L.L. & Polak, J.M. (2001). Gene-expression profiling of human osteoblasts following treatment with the ionic products of Bioglass, 45S5 dissolution, *Journal of Biomedical Materials Research Part A*, 55, 151-157.
- Yucel, S., Ozçimen, D., Terzioğlu, P., Acar, S. & Yaman, C. (2013). Preparation of Melt Derived 45S5 Bioactive Glass from Rice Hull Ash and Its Characterization, *Advanced Science Letters*, 19, 3477-3481.